THE JOURNAL OF PHYSICAL CHEMISTRY A

 VOLUME 112, NUMBER 4, JANUARY 31, 2008

ARTICLES

The Hammett Relationship and Reactions in the Excited Electronic State: Hemithioindigo *Z*/*E*-Photoisomerization

Thorben Cordes,[†] Torsten Schadendorf,[‡] Beate Priewisch,[‡] Karola Rück-Braun,[‡] and Wolfgang Zinth*,[†]

Munich Center for Integrated Protein Science, CIPS[M], and Lehrstuhl für BioMolekulare Optik, Department für Physik, Ludwig-Maximilians-Universität München, Oettigenstrasse 67, 80538 München, Germany, and Technische Universität Berlin, Institut für Chemie, Strasse des 17. Juni 135, 10623 Berlin, Germany

Received: September 17, 2007; In Final Form: October 25, 2007

The photochemical reaction dynamics of a set of photochromic compounds based on thioindigo and stilbene molecular parts (hemithioindigos, HTI) are presented. Photochemical *Z*/*E* isomerization around the central double bond occurs with time constants of 216 ps ($Z \rightarrow E$) and 10 ps ($E \rightarrow Z$) for a 5-methyl-hemithioindigo. Chemical substitution on the stilbene moiety causes unusually strong changes in the reaction rate. Electron-donating substituents in the position para to the central double bond (e.g., *para*-methoxy) strongly accelerate the reaction, while the reaction is drastically slowed by electron-withdrawing groups in this position (e.g., *para*-nitrile). We correlate the experimental data of seven HTI-compounds in a quantitative manner using the Hammett equation and present a qualitative explanation for the application of ground-state Hammett constants to describe the photoisomerization reaction.

1. Introduction

The rapid progress in the field of time-resolved spectroscopy allows us to gain deep insight into the fastest processes of photochemical reactions. The field of femtochemistry combines the manipulation of photochemical processes using light with the detailed investigation of the reaction steps.[1] Immediately after absorption of a photon, fast motions bring the system away from the initially populated Franck−Condon region. This motion is most likely controlled by the slope of the potential energy surface and may be related to the observation of oscillatory features in the ultrafast experiments. Some strongly driven reactions, such as the *Z*-to-*E* photoisomerizations of stilbene or azobenzene occur on time scales of a few hundred femtoseconds.[2] Here, the special shape of the potential energy surface guides the nuclear motion toward the transition region and facilitates rapid and efficient formation of the photoproduct in its electronic ground state.[3] For slower photochemical reactions the relaxation of vibrational excess energy in the excited electronic state, which occurs within a few picoseconds, may considerably alter the reaction behavior. Instead of a fast driven motion on a steep potential energy surface, a diffusion-like behavior on a rough free energy landscape occurs. In this case, the reaction rate may be controlled by barriers on the free energy surface: the height of the barrier, which limits the access to the transition region, largely determines reaction speed and efficiency. While the manipulation of ultrafast reactions via coherent control is limited to reaction dynamics preceding vibrational relaxation, conventional parameters have to be used to influence slower photochemical processes. The barrier height of a specific reaction may be varied by substitution, the energy

* Corresponding author. Fax: (+49) 89-2180-9202. E-mail: zinth@physik.uni-muenchen.de.
[†] Ludwig-Maximilians-Universität.
[‡] Technische Universität Berlin.

10.1021/jp077472l CCC: $40.75
Published on Web 01/05/2008

required to cross the barrier can be supplied by an additional light pulse. In this context, linear free-energy relations (LFER) may be applied to describe the influence of systematic modifications of the excited-state reaction.[4−7] The concept of LFER, which is directly linked to the existence of an energetic barrier, was successfully applied in various fields of ground-state reaction kinetics to describe the consequence of a variation of reaction parameters. A most prominent example of a LFER in chemistry is the Hammett equation:[4]

$$\log\left(\frac{k_R}{k_H}\right) = \log\left(\frac{\tau_H}{\tau_R}\right) = \rho\sigma \qquad (1)$$

This empirical relation has originally been used to correlate the influence of substituents in the aromatic ring upon the acidity of benzoic acids.[4] Here, the reaction barrier mainly depends on the change of electron density in the reaction center. The specific substituent R, characterized by the Hammett parameter σ, is directly related to the reaction rate k_R. Within this equation k_R and k_H are the rate constants for a specific reaction of the substituted and unsubstituted derivative, respectively. Electronic properties, and consequently the chemical nature (e.g., donor/acceptor characteristics) and the position of a substituent R, are described by the Hammett parameter σ. Several sets of Hammett parameters have been introduced to treat reactions that are poorly described by the original constants.[4] Here, new correlation constants consider resonance or steric interactions[4] or may even describe processes in the excited electronic state.[5] The original σ constants are the sum of inductive and resonance effects of a certain substituent. When an electron-demanding reaction center is in resonance to the substituent, σ^+ constants best correlate these structure−reactivity relations.[4] The reactive site itself is characterized by a reaction constant ρ. This reaction constant measures the sensitivity of a specific reaction to substitution effects and additional external parameters, for example, solvent or temperature. The algebraic sign of the reaction constant indicates whether the reaction is nucleophilic ($\rho > 0$) or electrophilic ($\rho < 0$).

Nearly every chemical reaction has been treated via the original Hammett relation or with one of its extended forms to understand the related reaction mechanism or to optimize several reaction parameters for future experiments.[4] It remains an open question whether the Hammett relation can be applied to photochemical reactions (reactions occurring in the excited electronic state). The influence of substituents on photochemical reactions was found to differ from the one usually observed in ground-state chemistry.[6] This reason may have caused the introduction of $\sigma^{h\nu}$ parameters to describe substituent influences on a photochemical reaction.[5] In contrast to these studies, a few excited-state reactions were treated via the Hammett equation using ground-state constants.[7] In order to allow a clear connection between the photochemical reaction and the substitution pattern, a detailed analysis of the reaction dynamics is required. Since excited-state reactions often imply complex reaction pathways, the influence of substituents on a single reaction step needs to be studied in order to obtain a reasonable correlation. To meet these requirements, we have performed time-resolved absorption experiments, which allow us to monitor all intermediate states together with the formation of product states.[8]

The investigated hemithioindigo molecules (HTI, see Scheme 1), combining stilbene and thioindigo,[9,10] can undergo a photoinduced *Z*-to-*E* isomerization along the central carbon−carbon double bond. The photochemical conversion from the *Z*-form to the *E*-form is induced by ultraviolet light (400 nm), while visible light (∼500 nm) induces the $E \rightarrow Z$ isomerization. The present study details the influence of the stilbene substitution on single steps within the photoreaction. The influence of the substitution in the stilbene part of the molecule, affecting the reaction rate of the final isomerization step, is quantitatively described using the Hammett relation with known ground-state parameters, σ^+.

SCHEME 1: Chemical Structures of the Two Isomeric Forms of the Photoswitchable HTI Compounds[a]

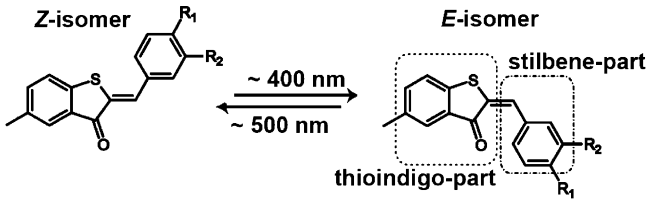

[a] The present study investigates seven HTI derivatives: R_1 = H, OMe, Cl, Br, CN with R_2 = H, R_2 = OMe, Br for R_1 = H. Near UV at ∼400 nm and visible light at ∼500 nm induce the isomerization processes.

2. Methods

Materials, Continuous Wave (cw)-Spectroscopy. The synthesis of the HTI derivatives (5-methylhemithioindigo derivatives) was conducted according to the procedures described in ref 9. All substances were dissolved in dichloromethane (Merck, purity 99,8%) with concentrations from 1 to 5 mM leading to an optical density of 2.0−2.5 at the *Z* isomer absorption maximum (1 mm optical path length). Two photostationary states were prepared for the femtosecond experiments: (i) A photostationary state containing approximately >95% *Z* isomer (HTI, Scheme 1, $R_1 = R_2 = H$) was generated by using the output of a cold-light source (KLC2500, Schott, Mainz, in combination with a 3 mm optical filter GG495, Schott) to investigate the $Z \rightarrow E$ isomerization. (ii) A photostationary state containing approximately 77% of the *E* isomer and 23% of the *Z* isomer (HTI, Scheme 1, $R_1 = R_2 = H$) was prepared using a mercury−xenon lamp (peaks at 400/430 nm, 3 mm thick optical filter GG385, Schott) to investigate the $E \rightarrow Z$ isomerization. The ratios of *Z*/*E* isomers were determined using NMR spectroscopy. Please note that the specific *Z*/*E* ratio varied slightly with substitution. Minor side reactions ([2 + 2] intermolecular cycloadditions) were observed for cw illumination of a mixture of the *Z*/*E* isomers over a very long time period (>20 h). During all femtosecond experiments, the initial composition (ratio of *Z*/*E* isomers) was kept constant by using one of the described illumination setups. A spectrophotometer (Perkin-Elmer, Lambda19) was used to measure the cw-UV/vis absorption spectra.

Time-Resolved Absorption Measurements. A home-built Ti:sapphire-based laser system delivered short pulses centered around 804 nm with a duration of 90 fs, a pulse energy of 1 mJ and a repetition rate of 1 kHz; for details, see elsewhere.[10−13] Excitation pulses for transient absorption measurements of the $Z \rightarrow E$ reaction were generated by doubling the fundamental in a BBO (type I) crystal to 402 nm. The $E \rightarrow Z$ reaction was investigated with pulses derived from a non-collinear optical parametric amplifier (NOPA[12]) optimized for the specific *E* absorption (∼490−515 nm). The pulses were tuned to the red part of the *E* isomer absorption spectrum, where the *Z* isomer showed no significant absorption. The excitation energies of the pump pulses varied between 200 and 400 nJ. A white light continuum generated in CaF_2[12] was used as probe light to monitor the transient absorption changes with the help of a multichannel detection system.[10−13] The probing process covered a spectral range from 350 to 650 nm. The pump and probe light were focused into the sample location (pump ∼150 μm, probe ∼40 μm) with polarization at magic angle. A chopper blocked

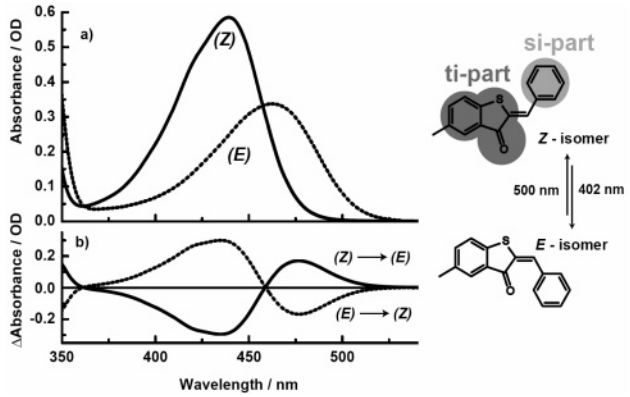

Figure 1. (a) Absorption spectra of the *Z* isomer (—) and *E* isomer (···) of the unsubstituted compound in dichloromethane. Panel b presents the absorbance changes induced by the two photoisomerization processes.

every second excitation pulse in order to improve referencing. During the femtosecond experiments, the sample solutions were pumped through a fused-silica flow cell with an optical path length of 0.5 mm, and the sample volume was completely exchanged between two consecutive laser pulses. Each data point was measured with repetitive scans (ca. 10) of the time delay between pump and probe and consisted of ∼10 000 averaged single laser shots. The transient background signal of the solvent was substracted from the sample signal. Time traces at each wavelength were corrected for the corresponding chirp of the white light continuum. All experiments were performed at room temperature.

Hammett Correlation. The procedure to evaluate the Hammett correlation uses a least-square algorithm as implemented in Origin 6.1. The quality of the correlation between the experimental rate constants and the empirical Hammett values (according to eq 1) is given by the correlation coefficient *R*. A value of $R = 1,-1$ corresponds to a perfect correlation depending on the slope, while $R = 0$ indicates no correlation.

3. Results

The absorption spectra of the unsubstituted *Z*/*E* isomers are presented in Figure 1a. Both isomers show overlapping absorption bands in the blue-green part of the visible spectrum. The maximum absorption of the *Z* and *E* isomer is found at $\lambda(Z)_{max} \approx 430$ nm and $\lambda(E)_{max} \approx 460$ nm, respectively. The peak extinction coefficient of the *E* isomer is smaller by a factor of 2 compared with the maximum absorption of the *Z* isomer. At room temperature, only the *Z* isomer is stable, while the *E* isomer reverts into the *Z* form on the time scale of several hours depending on the specific substitution pattern.[9] The absorbance changes (Figure 1b) resulting from the $Z \rightarrow E$ process show characteristic features with bleaching at 430 nm and absorption increase at 480 nm. The difference spectrum of the inverse process ($E \rightarrow Z$) is mirror symmetric. These spectroscopic data give no indications for the occurrence of side reactions.

In order to gain information about the kinetics of the isomerization, *Z* and *E* isomers of different HTI molecules are excited with ultrashort light pulses (∼100 fs) centered at 402 and 500 nm, respectively. The transient absorption (TA) data of the excited unsubstituted *Z* isomer is shown in Figure 2a. A broad excited-state absorption (ESA) modulated by ground-state bleaching (GSB, 430 nm) can be observed until the 100 ps time range. During the first 30 ps, changes in the shape of the transient spectra are observed. These can be assigned to kinetic processes involving excited electronic states. Later only the decay of the signal amplitude is seen. After 1 ns, a constant absorbance difference with bleaching at 430 nm and absorption

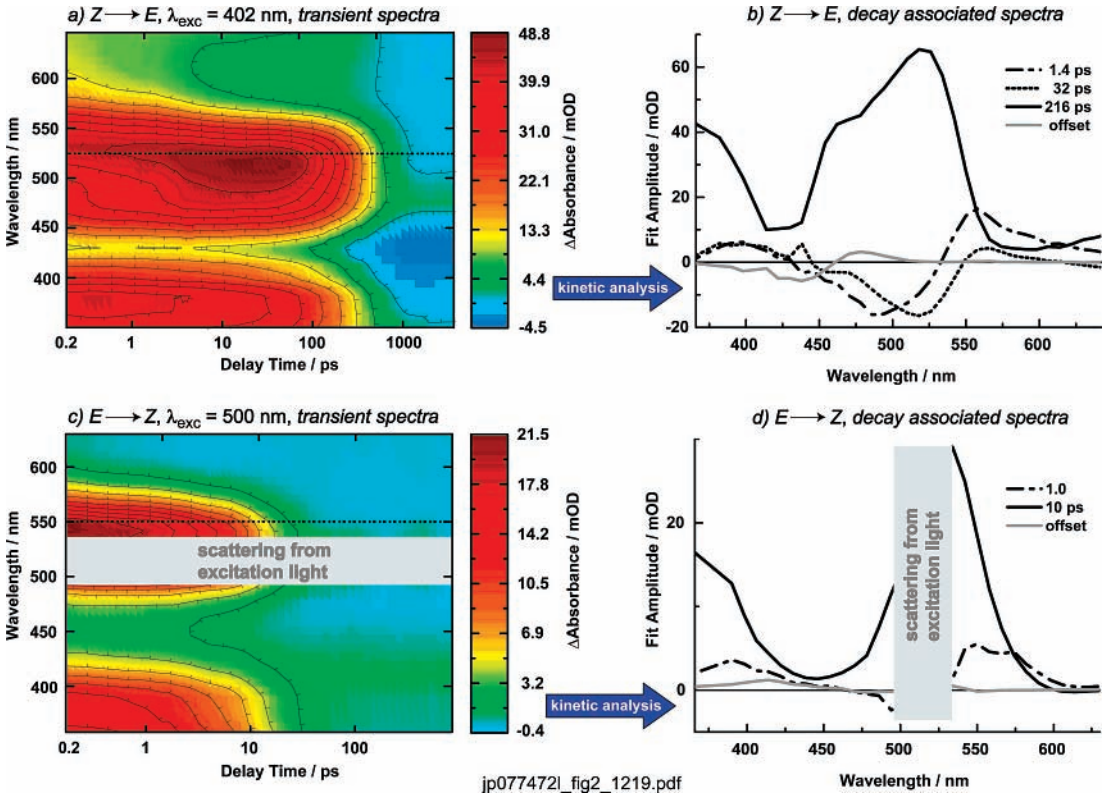

Figure 2. Transient absorption data of the unsubstituted HTI compound (Scheme 1, $R_1 = R_2 = H$) as a two-dimensional overview of the absorbance changes versus delay time for all detection wavelengths: (a) $Z \rightarrow E$ reaction; (c) $E \rightarrow Z$ reaction. Dotted slices indicate the detection wavelength shown for the comparison of different HTI compounds as described below. A kinetic analysis using a global fitting routine is shown for the respective data sets in panels b and d.

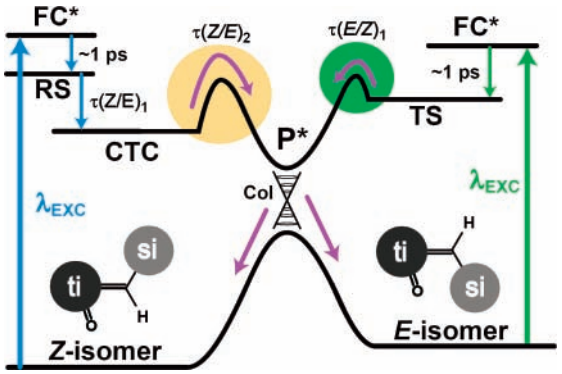

Figure 3. Simplified state models for both isomerization reactions ($Z \rightarrow E$, left; $E \rightarrow Z$, right) showing all important states together with their corresponding lifetime. The $Z \rightarrow E$ reaction consists of three steps, with the rate-determining step τ_2. The $E \rightarrow Z$ reaction is a sequential following of two states with the long-lasting time constant τ_1. Please note that only one P* is drawn to keep the clarity of the scheme. Different P* states may be involved in the two isomerization processes.

increase at 480 nm indicates product formation (compare with Figure 1b). A global fitting procedure allows us to describe the temporal behavior of the transients with time constants $\tau_0 = 1.4$ ps, $\tau_1 = 32$ ps, and $\tau_2 = 216$ ps. The decay-associated spectra (DAS) related to the time constants are shown in Figure 2b. These time constants describe three intermediate states during the HTI photoisomerization. The DAS of the time constants $\tau_0 = 1.4$ ps and $\tau_1 = 32$ ps are related to motions of the molecule on the excited-state potential surface. The final return to the ground state can be associated with the time constant $\tau_2 = 216$ ps. As shown in a former publication of a related HTI compound, these experimental observations are best described by a sequential reaction scheme.[13] Here, alternative reaction courses (e.g., branching) could be excluded using several time-resolved techniques (UV/vis, fluorescence, IR) combined with a theoretical modeling procedure.[13] The same number of time constants in the TA data and the large similarities of the DAS between the different HTI molecules motivate us to adapt the published sequential model[13] and to use the same interpretation for the observed TA data: A 400 nm photon generates a Franck−Condon state (FC*) with a large amount of excess energy (Figure 3, left). This state undergoes ultrafast energy dissipation, relaxation, and solvation processes resulting in the formation of a relaxed state (RS) on the time scale of $\tau_0 = 1.4$ ps. Within this time, the emission from the FC* state is red-shifted, which explains the negative amplitude at 490 nm and a positive amplitude at 560 nm seen in the DAS (Figure 2b, 1.4 ps). The structure of the molecule is not drastically changed, which conserves the oscillator strength. Subsequently the former central double bond starts to twist slightly and forms a state with a certain charge-transfer character (CTC), the time constant being τ_1. The transition from RS → CTC is connected with a loss of stimulated emission around 515 nm (Figure 2b, 32 ps), which is a well-known emission characteristic of twisted species.[13,14] These spectral features perfectly match the observation from former studies on related HTI molecules.[13] The final decay of the CTC state can be associated with the time constant τ_2. From this long time constant τ_2, we infer a barrier on the excited-state potential surface (Figure 3) that delays reaching a shorter-lived transition region (P*[15−17]) still on the excited-state surface, from where the ground state can be reached via a conical intersection (CoI)[18] in an ultrashort time. We can hence conclude that the rate-limiting step for product formation, the crossing of the barrier between CTC and P*, is related to the time constant τ_2, which is 216 ps for the $Z \rightarrow E$ process of the unsubstituted compound.

The $E \rightarrow Z$ isomerization process (Figure 2c) induced by 500 nm excitation occurs on faster time scales. Again the broad ESA is superimposed by GSB centered around 450 nm. The complete signal decays on the time scale of 10 ps. A constant absorbance difference with the characteristic features for product formation is found after 50 ps. A kinetic analysis results in a biexponential behavior of the transient data set with two time constants, $\tau_0 = 1.0$ ps and $\tau_1 = 10$ ps. The global analysis is plotted in Figure 2d. The molecules show spectral characteristics of relaxation processes on the time scale of τ_0. The scattering of excitation light in the range of the gray bar in Figure 2c,d complicates the interpretation of the corresponding DAS. The complete signal finally decays toward a long lasting absorbance difference due to product formation with the time constant τ_1.

As found in the case of the $Z \rightarrow E$ isomerization a Franck−Condon species (FC*) is immediately formed after photoexcitation of the *E* isomer. The molecule undergoes fast relaxation processes (Figure 3, right), which may lead to a partially twisted structure (TS) within 1 ps (τ_0). This 1 ps transition is only characterized by a small spectral shift as seen in the DAS in Figure 2d. The return to the ground state (τ_1) is again hindered by a barrier, which influences the access to the transition region. Here, a completely twisted structure (P*/CoI) gives efficient access to the ground state. The complete reaction model for both reactions is sketched in the simplified reaction scheme shown in Figure 3. It summarizes the experimental findings and the interpretations made above. Here, crossing of the potential barriers is the rate-limiting step for both isomerization directions. The existence of these barriers on the potential energy surface has been proven by temperature-dependent TA measurements for both photoreactions and will be discussed in a forthcoming publication.

We now turn to the substitution dependence of the isomerization reaction and study HTI derivatives with different substitution patterns. Figure 4 shows an overview of the absorption properties of all investigated para compounds for the lowest-energy transition. It can be seen that the absorption maximum of the *Z*/*E* isomers shows no systematic change due to substitution: both electron-donating (*p*-OMe, $\lambda(Z)_{max} = 448$ nm, $\lambda(E)_{max} = 473$ nm) and electron-withdrawing groups (e.g., *p*-Br, $\lambda(Z)_{max} = 442$ nm, $\lambda(E)_{max} = 466$ nm) are characterized by a moderate red-shift of the absorption band compared with the unsubstituted compound (*p*-H, $Z = 438$ nm, $E = 462$ nm). This means that the transition energy to the FC* state drops only slightly with substitution. As a consequence, the properties of the FC* state remain essentially unchanged.

In contrast to this nonsystematic and moderate influence on the absorption spectra, the substitution has a strong impact on the kinetics of both the $Z \rightarrow E$ and the $E \rightarrow Z$ reaction as seen in Figure 5a,b. The fastest reaction is observed for the methoxy-substituted derivative (*p*-OMe) and the slowest for the nitrile compound (*p*-CN). The characteristic reaction times are changed by more than 2 orders of magnitude. An acceleration of the reaction is achieved by electron-donating groups (Figure 5a,b, blue), while electron-withdrawing groups slow down the reaction kinetics (Figure 5a,b, green and red). To quantify these substitution effects, all data sets were globally fitted with multiexponential trial functions as described for the unsubstituted derivative (Figure 2). The transient data sets of the respective compounds require three ($Z \rightarrow E$) or two ($E \rightarrow Z$) exponential fit functions for a proper description of the experimental findings. The first time constant (τ_0) is always in the range of

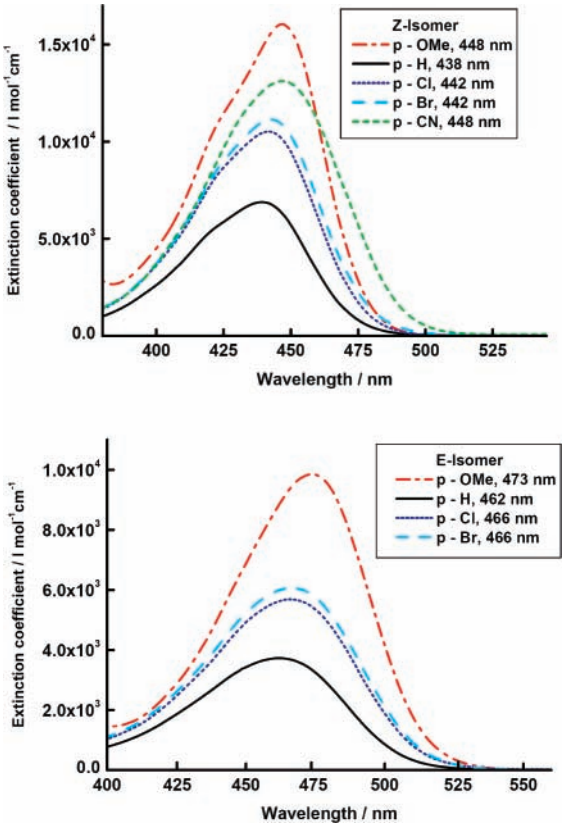

Figure 4. Absorption properties of the different *para*-substituted *Z* isomers (top panel) and *E* isomers (bottom panel). The peak positions of the lowest energy transition ($S_0 \rightarrow S_1$) are given in the insets.

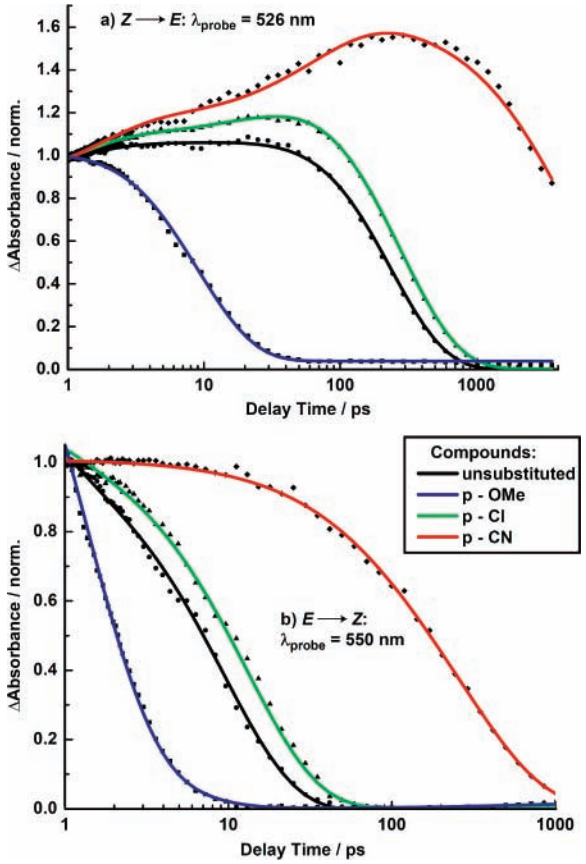

Figure 5. Comparison of different *para*-substituted HTI molecules in dichloromethane. The figure shows an excerpt of the transient data set at a certain detection wavelength as pointed out in Figure 2. The absorbance changes are normalized at a delay time of 1 ps. The experimental data points are shown together with their corresponding fit function: (a) $Z \rightarrow E$, $\lambda_{probe} = 526$ nm; (b) $E \rightarrow Z$, $\lambda_{probe} = 550$ nm.

a few picoseconds and shows no significant change due to substitution. The time constants τ_1, τ_2 ($Z \rightarrow E$), and τ_1 ($E \rightarrow Z$) vary with substitution as listed in Table 1 and refer to the photochemical steps shown in Figure 3. The spectral shape of the decay-associated spectra (DAS) related to these time constants does not depend on substitution, which indicates that the number and type of intermediates remain constant compared with the unsubstituted compound. The similar patterns in the DAS of all compounds show that substitution has no impact on the reaction mechanism while it does influence the reaction rate. Alternative reaction pathways via a triplet manifold as found for halogenated stilbenes[4,19] or thioindigo[20] do not show up significantly in the experiments of the studied HTI compounds. So, all different compounds react via a singlet mechanism and should follow a sequential route back to the ground state as detailed in Figure 3.

TABLE 1. Lifetime Values for Both Isomerization Processes (Solvent Dichloromethane)[a]

	$Z \rightarrow E$		$E \rightarrow Z$	Hammett constant	
derivative	τ_1, ps	τ_2, ps	τ_1, ps	σ	σ^+
OMe (para)	5.2	11.8	1.2	−0.28	−0.78
H	30	216	10.1	0	0
OMe (meta)	28	245	11.6	0.1	0.05
Cl (para)	38	269	13.1	0.23	0.11
Br (para)	40	336	19.1	0.26	0.15
Br (meta)	45	1480	36	0.37	0.41
CN (para)	72	2650	300	0.7	0.66

[a] The time constants τ_2 ($Z \rightarrow E$) and τ_1 ($E \rightarrow Z$) are related to product formation. A fast component τ_1 ($Z \rightarrow E$) corresponds to the formation of the intermediate CTC state. Errors for the lifetimes are ±20%. The compounds are listed by increasing Hammett constants taken from ref 4f.

4. Discussion

In order to test whether a LFER applies to the photochemical reactions of the HTI compounds, the different time constants (reaction rates) are plotted in Figure 6 as a function of the Hammett parameters σ and σ^+. The Hammett correlations for the $Z \rightarrow E$ process (product formation, τ_2) are shown in Figure 6a,b. Here, the plot results in a linear behavior with a reasonable correlation coefficient of $R = -0.944$ when using σ parameters (Figure 6a). A considerably better correlation of $R = -0.995$ is found for σ^+ parameters (Figure 6b). In addition, we note that all compounds closely follow the linear relation (Figure 6b). This supports a common reaction mechanism for the $Z \rightarrow E$ isomerization. It is well-known from ground-state reactions that the situation of direct conjugation of a pair of electrons at the α position of the substituent with the reaction site in the transition state is better described by σ^+ values rather than σ values.[4] The observed substituent effects indicate that the product formation during $Z \rightarrow E$ isomerization of HTI molecules occurs via a partially charged transition state with an electron-demanding reaction center and effective delocalization of a small positive charge.[4] The same analysis was applied to the formation time of the CTC state (τ_1, plot not displayed). Here correlation coefficients of $R = -0.978$ and $R = -0.902$ are obtained using the σ^+ and the σ parameters, respectively. The better fit of the σ^+ parameters suggests that similar conclusions as presented above may be drawn about the nature of the transition region separating TS from CTC. However the ρ values (see eq 1) of the two reactions differ considerably: $\rho = -0.78$ ($Z \rightarrow E$, τ_1,

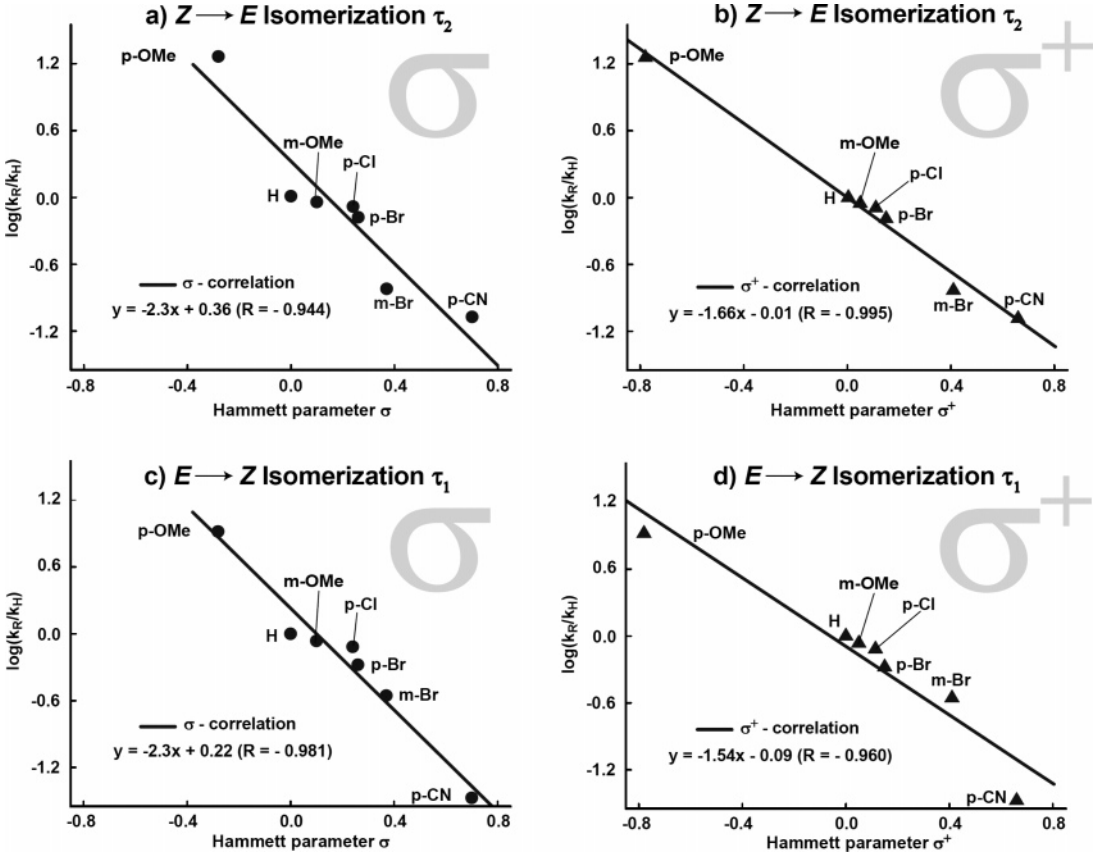

Figure 6. Hammett correlation for the two isomerization processes: (a, b) Hammett correlation for the $Z \rightarrow E$ reaction using σ (a) and σ^+(b); (c, d) Hammett correlation for the $E \rightarrow Z$ reaction using σ (c) and σ^+(d). The reaction constants can be referred to the slope of the linear relation as indicated in the lower part of each panel. R corresponds to the absolute value of the correlation coefficient and describes the fitness of the correlation.

not displayed) and $\rho = -1.66$ ($Z \rightarrow E$, τ_2, Figure 6b). Because the absolute value of the reaction constant ρ for the decay of the CTC state is 2-fold larger than the one for the decay of TS, it can be concluded that the sensitivity to polar substituents increases during the motion of the photoexcited Z isomer on the potential energy surface. So, the photoexcited Z isomer is transformed into a more polar species in the course of the reaction.

The analysis of the product formation for the $E \rightarrow Z$ isomerization is shown in Figure 6c,d. A value of $R = -0.981$ (Figure 6c) is found for the σ correlation compared with $R = -0.960$ for the σ^+ correlation (Figure 6d). Prior to a further discussion of the molecular implications of these findings, we have to confirm that the major prerequisite for the validity of the Hammett equation, namely, a constant reaction mechanism for all compounds, is still fulfilled. For reaction times longer than a few picoseconds, we can assume that an excited-state reaction is controlled by barriers on the excited-state free energy surface. Since all time constants for the $Z \rightarrow E$ isomerization are longer than 5 ps (see Table 1), the assumption is valid for all compounds in this case. On the other hand, the *para*-methoxy derivative has a very short reaction time $\tau_1 = 1.2$ ps for the $E \rightarrow Z$ reaction. We now return to the analysis of the Hammett correlation of the $E \rightarrow Z$ isomerization: Removing the time constant of *para*-methoxy (*p*-OMe) from the data set, we end up with similar correlation coefficients of $R = -0.970$ (σ^+) and $R = -0.964$ (σ). On the other hand, one may also test the outcome of Hammett correlations for a data set where the slowest (*para*-nitrile, *p*-CN) derivative is removed while keeping the *para*-methoxy data. Here a nearly perfect σ^+ correlation with $R = -0.997$ is obtained whereas the σ correlation remains at $R = 0.962$. For the $E \rightarrow Z$ isomerization, we may conclude that a good qualitative correlation exists for the σ and the σ^+ Hammett parameters. However we are not able to decide whether the σ or the σ^+ correlation should be preferred.

The successful Hammett correlations for all investigated reaction steps show that a pronounced structure−reactivity relation exists for all investigated HTI compounds. Both reactions ($Z \rightarrow E$, $E \rightarrow Z$) proved to be highly sensitive to substitution; the observed effects comprise more than 2 orders of magnitude in time. A quantitative correlation between the empirically derived Hammett constants and the HTI reaction rates was shown and analyzed. The use of ground-state σ^+ values resulted in valuable correlations, which is surprising for a reaction occurring in the excited state. The question remains why ground-state properties seem to control the photochemical course of the HTI molecules.

The reaction rate of HTI photoisomerization is determined by the access to the transition region (P*/CoI) via a barrier between CTC/TS and P* as pointed out in Figure 3. Here, the properties of the key intermediate P* can be used to explain the correlation between ground-state Hammett values and the HTI reaction rate in the excited state. For this purpose, we refer to the known model for the photoisomerization of stilbene as an analog for HTI. An early approach to describe the photoisomerization of stilbene is given by Saltiel and Orlandi[16] who suggested a model with two excited-state potential surfaces and a simplified reaction coordinate, that is, the rotation around the central double bond with a dihedral angle ϕ. These early models have been extended by Hohleichner.[16b] More recent considerations of stilbene potentials can be found in Fuss et al.[18] The important characteristics are shown in Figure 7a. The electronic

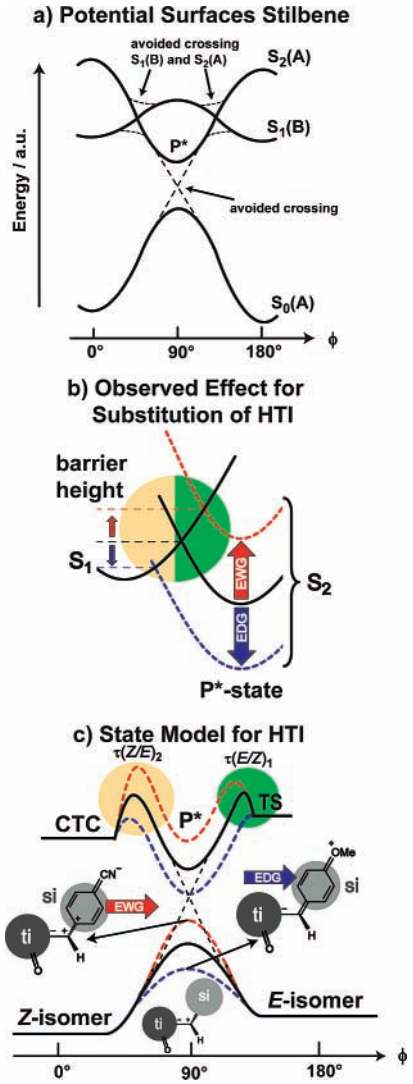

Figure 7. Schematic reaction profiles: (a) Orlandi−Siebrand model of the potential energy surfaces of stilbene;[16,17] (b) proposed mechanism for the change in barrier height for varying substitution for HTI; the barrier on the excited-state potential surface is decreased or increased according to the electronic nature of the substituent; (c) a possible explanation for the substitution effect is a change in the energetic location of the avoided crossing, which shifts the energetic position in the ground and excited state in a similar manner. Two possible resonance structures of the 90° twisted state (in the electronic ground state) are shown for different substitution on the stilbene part. Their charge distribution supports the idea that the energetic position of the 90° twisted state in the ground and excited state strongly depends on the specific substitution pattern (shown schematically by the red and blue curves). It has to be noted that the P* state does not need to be common for both isomerization directions. (The energy of the states is not to scale. EWG = electron-withdrawing group; EDG = electron-donating group; ti = thioindigo part; si = stilbene part).

ground state S_0(A) is described by a potential curve with two minima at $\phi = 0°$, 180° and a maximum at $\phi = 90°$. The one-electron excited state S_1(B) exhibits again two minima at $\phi = 0°$, 180° and a maximum at $\phi = 90°$. Its potential energy curve crosses the doubly excited state S_2(A), which has two maxima at $\phi = 0°$, 180° and a minimum at $\phi = 90°$. Avoided crossings of S_1(B) and S_2(A) surfaces result in the formation of barriers on the excited-state potential surface. The photochemical reaction may proceed as follows: after excitation to the S_1(B) state, the molecule may twist around its double bond and gains access to the minimum at $\phi = 90°$ (P*) only if it is able to overcome this barrier. A conical intersection near to P* allows effective and fast (much less than a few picoseconds) repopulation of the ground state with branching into educt and product. The time scale of the complete photoreaction is determined by the barrier formed by avoided crossing of S_1(B) and S_2(A) limiting the accessibility of P*/CoI.

We adapt this concept to the HTI molecules and assume that two excited states, S_1 and S_2, exist and are important for the photoisomerization (for HTI these states cannot be assigned to A or B due to the asymmetry of the HTI molecule). It is likely that S_1 and S_2 state energies are influenced by substitution.[21] At first, we assume for the vicinity of the transition region that the energy of the S_2 state is more strongly influenced by substitution: this is shown in Figure 7b where the energetic position of the P* minimum drops for compounds with electron-donating groups and is increased for electron-withdrawing groups. This results in a change in the height of the reaction barrier and is in agreement with the trend observed experimentally. The assumptions made above (Figure 7b) are supported by the known behavior of stilbene.[21] On the S_0 and the S_2 surfaces, these molecules acquire a biradicaloid/zwitterionic form in the vicinity of $\phi = 90°$. We now assume that this behavior also applies to HTI. Here again the P* minimum and the maximum of the potential energy curve in the ground state at $\phi = 90°$ due to an avoided crossing (Figure 7c, black curve). When the central double bond in the electronic ground state is twisted by $\phi = 90°$, the electronic structure can be represented by a zwitterionic species.[2,17,21] Due to the asymmetry of the HTI molecules, the negative charge of the zwitterion is more likely oriented toward the electron-withdrawing oxygen within the thioindigo part and the positive charge is located at the central C atom in the vicinity of the substituted phenyl ring (see resonance structure in Figure 7c, lower part). This state can be stabilized by an electron-donating group attached to the stilbene part, which tends to compensate the positive charge (methoxy compound). When electron density is removed from the ring system (nitrile compound), a "second positive charge" can be found for one possible resonance structure, and the energy increases.

The energetic changes in the vicinity of the $\phi = 90°$ structure have severe consequences for the barriers encountered upon isomerization: (i) In the electronic ground state, the barrier between the *Z* form and the *E* form is increased for electron-withdrawing substituents on the stilbene part. This influences the thermal relaxation of the *E* isomer in the ground state. (ii) In the excited electronic state, the energetic position of P* is influenced in the same way as found for the ground-state twisted structure. If electron density is removed from the stilbene part by an electron-withdrawing group, the energetic position of P* is raised, which also increases the barrier height for the excited-state reaction. Lowering its energy by introducing an electron-donating group consequently decreases the barrier height and leads to the observed trend in the photochemical reaction rates.

5. Conclusion

We have investigated the *Z*/*E* photoisomerization of several HTI compounds with variations in the stilbene substitution pattern. A reaction model for both isomerization processes of 5-methyl-hemithioindigos was shown and analyzed. The effect of stilbene substitution was detailed; a drastic influence of the substitution pattern is found on the reaction rates of both the $E \rightarrow Z$ and the $Z \rightarrow E$ direction. The changes in the reaction time could be successfully correlated using the Hammett equation with the ground-state Hammett constants, σ^+. A

qualitative molecular interpretation based on excited-state potential surfaces and a simplified reaction coordinate in analogy to the descriptions of the photoisomerization of stilbene explains the correlation between ground-state Hammett constants and the HTI reactivity in the excited electronic state. The known Hammett constants σ and σ^+ should also allow one to predict and to control the reaction rate of compounds with a related reaction mechanism.

Acknowledgment. T.C. gratefully acknowledges a scholarship donated by the "Fond der chemischen Industrie". We thank P. Gilch for careful reading of the manuscript, helpful discussions, and critical comments. The work was supported by Deutsche Forschungsgemeinschaft (Grant SFB533, B9). K.R.-B. wishes to thank the Deutsche Forschungsgemeinschaft (Grants SFB 498 and SFB 658), the Volkswagen Foundation, and the Fonds der Chemischen Industrie for financial support.

References and Notes

(1) Castleman, A. W., Jr.; Kimble, M. L. *Femtochemistry VII: Fundamental Ultrafast Processes in Chemistry, Physics, and Biology*; Elsevier: Amsterdam, 2006.

(2) (a) Saltiel, J.; Sun, Y. P. In *Photochromism, Molecules and Systems*; Dürr, H., Bouas-Laurent, H. Eds.; Elsevier: Amsterdam, 1990; p 64 ff. (b) Waldeck, D. H. *Chem. Rev.* **1991**, *91*, 415−436. (c) Meier, H. *Angew. Chem., Int. Ed. Engl.* **1992**, *31*, 1399−1450. (d) Dugave, C.; Demange, L. *Chem. Rev.* **2003**, *103*, 2475−2532. (e) Görner, H.; Kuhn, H. J. *Adv. Photochem.* **1995**, *19*, 1−117.

(3) Nägele, T.; Hoche, R.; Zinth, W.; Wachtveitl, J. *Chem. Phys. Lett.* **1997**, *272*, 489−495.

(4) (a) Hammett, L. P. *Chem. Rev.* **1935**, *17*, 125−136. (b) Hammett, L. P. *J. Am. Chem. Soc.* **1937**, *59*, 96−103. (c) Jaffee, H. H. *Chem. Rev.* **1953**, *53*, 191−261. (d) Wells, P. R. *Chem. Rev.* **1963**, *63*, 171−219. (e) Hansch, C.; Taft, R. W. *Chem. Rev.* **1991**, *91*, 165−195. (f) Smith, M. B.; March, J. *March's Advanced Organic Chemistry*, 5th ed.; Wiley-Interscience: New York, 2001. (g) Williams, A. *Free Energy Relationships in Organic and Bio-Organic Chemistry*; The Royal Chemical Society: Cambridge, UK, 2003.

(5) McEwen, J.; Yates, K. *J. Phys. Org. Chem.* **1991**, *4*, 193−206.

(6) (a) Zimmermann, H. E.; Schuster, D. I. *J. Am. Chem. Soc.* **1961**, *83*, 4486−4488. (b) Zimmermann, H. E.; Sandel, V. R. *J. Am. Chem. Soc.* **1963**, *85*, 915−922. (c) Zimmermann, H. E.; Somasekhara, S. *J. Am. Chem. Soc.* **1963**, *85*, 922−927.

(7) (a) Papper, V.; Pines, D.; Likhtenshtein, G.; Pines, E. *J. Photochem. Photobiol. A* **1997**, *111*, 87−96. (b) Papper, V.; Likhtenshtein, G. I. *J. Photochem. Photobiol. A* **2001**, *140*, 39−52.

(8) Tamai, N.; Miyasaka, H. *Chem. Rev.* **2000**, *100*, 1875−1890.

(9) (a) Steinle, W.; Rück-Braun, K. *Org. Lett.* **2003**, *5*, 141−144. (b) Lougheed, T.; Borisenko, V.; Hennig, T.; Rück-Braun, K.; Wooley, G. A. *Org. Biomol. Chem.* **2004**, *19*, 2798−2801. (c) Herre, S.; Steinle, W.; Rück-Braun, K. *Synthesis* **2005**, *19*, 3297−3300.

(10) Cordes, T.; Weinrich, D.; Kempa, S.; Riesselmann, K.; Herre, S.; Hoppmann, C.; Rück-Braun, K.; Zinth, W. *Chem. Phys. Lett.* **2006**, *428*, 167−173.

(11) Spörlein, S.; Carstens, H.; Satzger, H.; Renner, C.; Behrendt, R.; Moroder, L.; Tavan, P.; Zinth, W.; Wachtveitl, J. *Proc. Natl. Acad. Sci. U.S.A.* **2002**, *99*, 7998−8002.

(12) (a) Huber, R.; Satzger, H.; Zinth, W.; Wachtveitl, J. *Opt. Commun.* **2001**, *194*, 443. (b) Seel, M.; Wildermuth, E.; Zinth, W. *Meas. Sci. Technol.* **1997**, *8*, 449−452.

(13) Cordes, T.; Heinz, B.; Regner, N.; Hoppmann, C.; Schrader, T. E.; Summerer, W.; Rück-Braun, K.; Zinth, W. *ChemPhysChem* **2007**, *8*, 1713−1721.

(14) (a) Rettig, W. *Angew. Chem., Int. Ed. Engl.* **1986**, *25*, 971−988. (b) Baumann, W.; Bischof, H.; Frohling, J. C.; Brittinger, C.; Rettig, W.; Rotkiewicz, K. *J. Photochem. Photobiol. A* **1992**, *64*, 49−72.

(15) (a) Saltiel, J. *J. Am. Chem. Soc.* **1967**, *89*, 1036−1037. (b) Saltiel, J. *J. Am. Chem. Soc.* **1968**, *90*, 6394−6400.

(16) (a) Orlandi, G.; Siebrand, W. *Chem. Phys. Lett.* **1975**, *30*, 352−354. (b) Hohleichner, G.; Dick, B. *J. Photochem.* **1984**, *27*, 215−231.

(17) Klessinger, M.; Michl, J. *Excited States and Photochemistry of Organic Molecules*, 1st ed.; VCH: New York, 1995.

(18) (a) Fuss, W.; Kosmidis, C.; Schmid, W. E.; Trushin, S. A. *Angew. Chem., Int. Ed.* **2004**, *43*, 4178−4182. (b) Fuss, W.; Kosmidis, C.; Schmid, W. E.; Trushin, S. A. *Chem. Phys. Lett.* **2004**, *385*, 423−430.

(19) (a) Saltiel, J.; Marinari, A.; Chang, D. W. L.; Mitchener, J. C.; Megarity, E. D. *J. Am. Chem. Soc.* **1979**, *101*, 2982−2996. (b) Görner, H.; Schulte-Frohlinde, D. *J. Phys. Chem.* **1979**, *83*, 3107−3118.

(20) Meada, Y.; Okada, T.; Mataga, N.; Irie, M. *J. Phys. Chem.* **1984**, *88*, 1117−1119.

(21) (a) Bonačić-Koutecký, V.; Koutecký, J.; Michl, J. *Angew. Chem., Int. Ed. Engl.* **1987**, *26*, 170−189. (b) Saltiel, J.; Ko, D. H.; Fleming, S. A. *J. Am. Chem. Soc.* **1994**, *116*, 4099−4100.